ACS OMEGA

Open Access

http://pubs.acs.org/journal/acsodf

Article

Allosteric Probe Recognition-Induced Exponential Amplification Reaction for Label-Free Photosensitization Colorimetric Detection of Small Extracellular Vesicles

Can Wu,[‖] Jingjun Xie,[‖] and Yuyu Chen*

Cite This: *ACS Omega* 2025, 10, 11498−11504

Read Online

ACCESS | Metrics & More | Article Recommendations | Supporting Information

ABSTRACT: The expression levels of small extracellular vesicles (sEVs) are acknowledged as highly promising diagnostic biomarkers for a variety of diseases, including chronic obstructive pulmonary disease and lung cancer. However, a convenient and sensitive system for on-site rapid detection of sEVs is still highly desired. We have created a portable and highly efficient photosensitization colorimetric platform for label-free, sensitive, and colorimetric sEV detection by using an allosteric probe to specifically identify the CD63 protein on the surface of sEVs, which triggers numerous signal cycles to generate color changes. Visual detection of sEVs could be accomplished in 60 min using this detection platform. It was noted that this detection platform was capable of effectively detecting the target at a concentration as low as 1.21 particles/μL, and the reaction was completed in a single step. The proposed assay could be potentially engineered to serve as a universal bioassay platform for the detection of other molecules when used in conjunction with other aptamers for probe design. The principle of this strategy is highly versatile and sensitive, making it accessible for a variety of biosensor developments and applications.

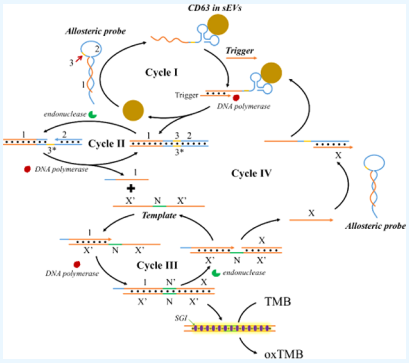

1. INTRODUCTION

Chronic obstructive pulmonary disease (COPD) is a treatable and preventable disorder distinguished by chronic ventilation obstruction and chronic respiratory symptoms.[1,2] The progression of COPD is influenced by a variety of factors, but inflammation serves as the primary indicator of the disease. By transmitting signals to target cells in a variety of ways, small extracellular vesicles (sEVs) may influence the expression process of DNA and microRNA (miRNAs) in recipient cells, thereby influencing the physiological and pathological processes of COPD.[3−5] The sEVs are implicated in the development and progression of numerous diseases and are regarded as novel regulators of COPD progression.[6,7] sEVs possess a lipid bilayer structure that serves to safeguard exosomal RNA against degradation by body fluid RNase. As a consequence, sEVs are more accurately able to mirror physiological changes occurring in the parent cells.[8] As a result, the development of technology for sensitive sEV detection is crucial for the pathological investigation and early detection of COPD and lung malignancies.

Traditionally, several techniques have been developed to evaluate the surface protein of sEVs, including Western blot and magnetic bead-based approaches.[9−11] Nevertheless, these techniques require a significant amount of time and multiple experimental procedures, making the process both time-consuming and labor-intensive. Furthermore, the immunoassay serves as a crucial approach for sEV detection with higher specificity, in which method-specific antigens on the surface of sEVs are detected and identified by antibodies. Two commonly used immunological techniques are the enzyme-linked immunosorbent assay (ELISA) and immunofluorescence assay. However, these procedures are time-consuming and susceptible to producing false-positive results. Compared to the investigation of sEVs using antibodies, aptamer-based detection approaches offer a straightforward and efficient approach to assessing the expression level of sEVs.[12−16] In recent years, several approaches for detecting sEVs by using aptamers have been developed. These methods combine aptamer-based target recognition with diverse signal amplification strategies, including rolling circle amplification (RCA),[17,18] recombinase polymerase amplification (RPA),[19] and catalytic hairpin assembly (CHA).[20−22] Nevertheless, these signal amplification solutions possess the limitations of intricate primer design, suboptimal amplification effectiveness, and the need for tagging a fluorescent moiety that is susceptible to experimental circumstances. Exponential amplification reaction (EXPAR) is an isothermal approach that efficiently amplifies small DNA and RNA fragments using DNA polymerase and nicking endonuclease.[23,24] In a typical

Received: January 1, 2025
Revised: February 16, 2025
Accepted: February 20, 2025
Published: March 10, 2025

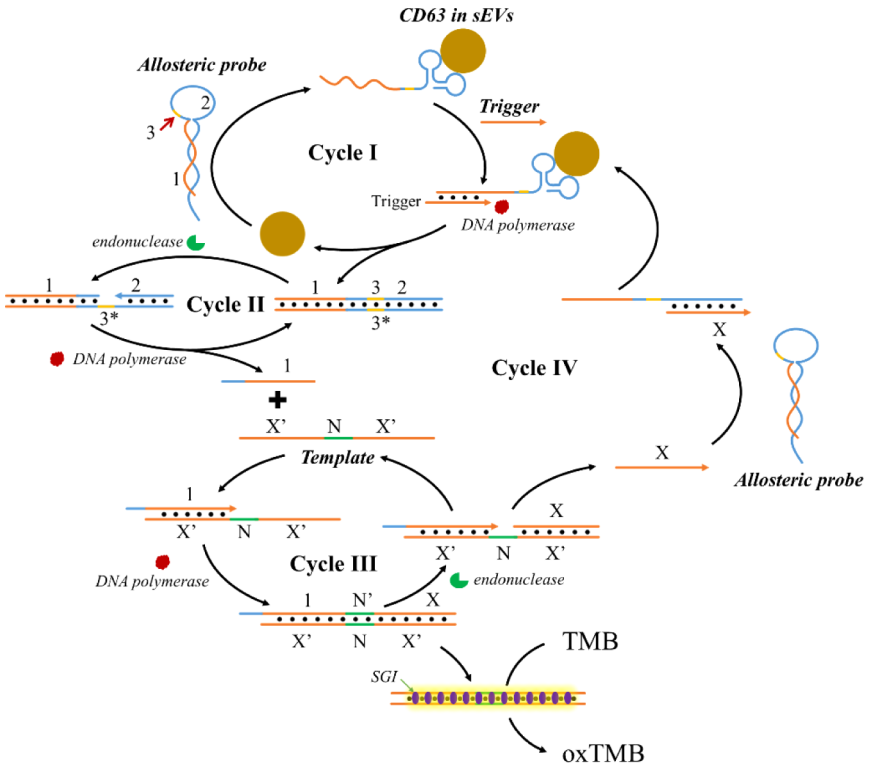

Figure 1. Design of the allosteric probe and four signal cycles for CD63 protein analysis on sEVs.

EXPAR, the trigger DNA binds to a template strand and elongates along the template strand with the assistance of a DNA polymerase. Next, the nicking endonuclease identifies the particular region on the elongated strand, generating a nicking site and displacing the newly formed strand in the next chain extension process. Subsequently, the displaced strand forms a hybrid with another template strand, initiating the subsequent cycle of reaction. EXPAR is a real-time technology that has been acknowledged for its exceptional amplification rate, ranging from 10^6 to 10^8 within 30 min. More importantly, the EXPAR is highly effective in producing a large amount of double-stranded DNA (dsDNA).[25,26]

In this work, we designed a strategy that utilizes an allosteric probe to specifically bind with the CD63 protein on the surface of sEVs, inducing four signal cycles to produce substantial double-stranded DNA probed by SYBR Green I (SGI). Taking the unique role of SGI as a photosensitizer and TMB as a chromogenic substrate,[27,28] the number of sEVs could be calculated by observing the color changes or the absorbance intensity (Figure 1). In this method, the allosteric probe is designed with a hairpin structure, containing three functional sections: "1" provides a binding site for the trigger sequence, "2" is the CD63 aptamer, and "3" is the endonuclease binding site. In the presence of sEVs, the "2" section binds with the CD63 protein, thus leading to the allosterism of the probe, exposing the "1" and "3" sections. The trigger sequence hybridizes with the "1" section and works as a primer to mediate chain elongation under the assistance of DNA polymerase, in which process the sEV cell is released to induce the next signal cycle (Cycle I). During Cycle I, a dsDNA product was generated containing the "3" (endonuclease binding site). Endonuclease recognizes the "3" section and generates a nicking site. Under the cooperation of endonuclease and DNA polymerase, Cycle II was conducted, generating a large amount of "1" sequence. The "1" sequence initiates the EXPAR process (Cycle III) to produce numerous X sequences and dsDNA products. In detail, the "1" section binds with the X′ in the template sequence and works as a primer to mediate chain extension under the assistance of DNA polymerase, transcribing the N′ section. The endonuclease can identify and cleave the N′ section to generate a nicking site. With the cooperation of DNA polymerase and endonuclease, a large number of X sequences that share the same sequence with "1" is produced. The X sequence can bind with the X′ in the template sequence to mediate EXPAR with the cooperation of DNA polymerase and endonuclease. In addition, the "X" has a more complementary section with the "2" section in the allosteric probe, which will unfold the allosteric probe to form Cycle IV. As a result, the target-induced transformation allows the quantitative amplification and preservation of dsDNA as a final product in the solution. By adding SGI as a photosensitizer and TMB as a chromogenic substrate, we can quantify the sEVs in a label-free and colorimetric manner.

2. METHODS AND MATERIALS

2.1. Reagents and Materials. The complete list of oligonucleotides used in this research can be found in Table S1. The sequences were synthetically produced and purified by Sangon Biotechnology Co., Ltd. (Shanghai, China). The CD9 protein, C-reactive protein (CRP), and bovine serum albumin (BSA) were acquired from Sigma-Aldrich (Beijing, China). SYBR Green I (SGI, 10000×) and 3,3′,5,5′-tetramethylbenzidine (TMB) were bought from Thermo Fisher Scientific (Beijing, China). Nt.BstNBI, Bst 2.0 WarmStart DNA polymerase, dNTPs, and SYBR Green I (SGI) were supplied by New England Biolabs (MA, U.S.A.). The Hitachi F-7100 Fluorescence Spectrophotometer from Japan was utilized to

https://doi.org/10.1021/acsomega.5c00016
ACS Omega 2025, 10, 11498−11504

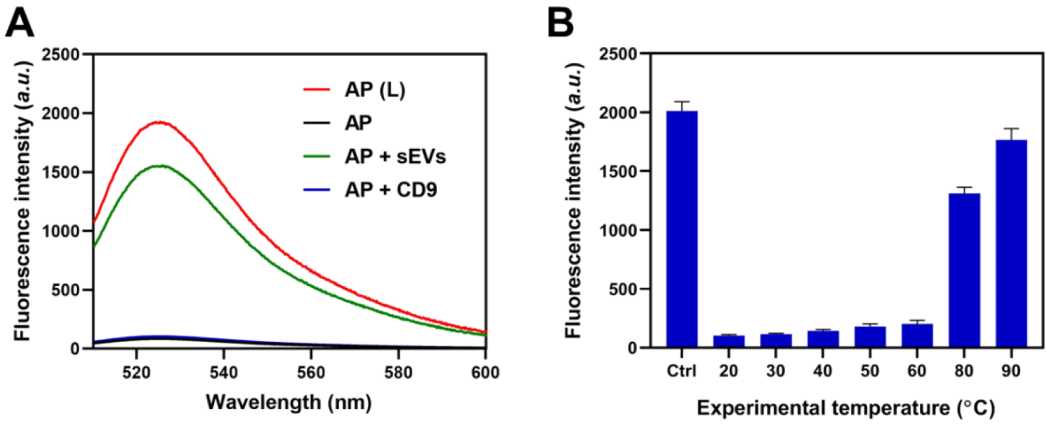

Figure 2. Construction of the allosteric probe. (A) Fluorescence intensity of the allosteric probe (AP) when sEVs or CD9 protein existed. AP (L), allosteric probe in the linear state. (B) Fluorescence intensity of the allosteric probe with different incubation temperatures. Control group (Ctrl), allosteric probe in a linear state.

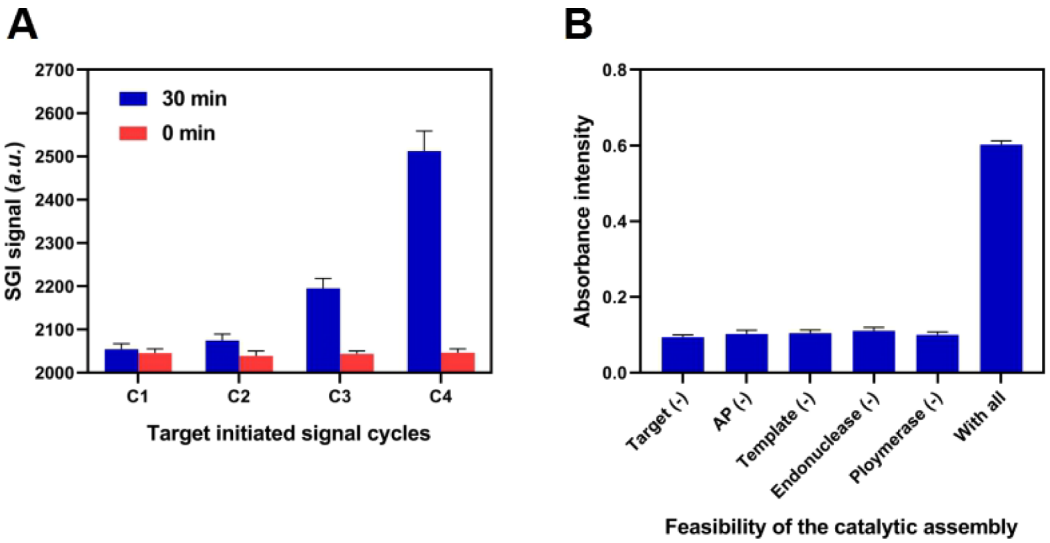

Figure 3. The feasibility of the target recognition-induced signal cycle. (A) SGI signals of the dsDNA product during the signal cycle. C1, allosteric probe (AP); C2, AP + primer; C3, AP + primer + DNA polymerase; C4, AP + primer + DNA polymerase + endonuclease. (B) Absorbance intensities of the method when essential experimental components existed or not.

obtain fluorescence spectra. The excitation and emission slit widths were both configured to 10 nm. The UV-3310 UV−vis spectrophotometer (Rili, Japan) was used in this research to record the UV−vis absorption spectra and calculate the peak absorbance value with a 10 mm path length cuvette at room temperature. Ten × PBS buffer solution was obtained from Sangon Biotechnology Co., Ltd. (Shanghai, China).

2.2. Preparation of Allosteric Probe. The synthesized allosteric probe in a linear state was dissolved in PBS buffer to a concentration of 5 μM. The mixture was then heated to 95°C for 5 min. Subsequently, the hairpin structure was formed through a self-assembly process by gradually cooling it to room temperature (RT).

2.3. Detection Performance of the Biosensor. 100 μL of sEVs with different concentrations were mixed with 10 μL of allosteric probe (500 nM), and the mixture was incubated at room temperature for 25 min. Afterward, 10 μL of trigger sequence (500 nM), 10 μL of template sequence for EXPAR (1 nM), 2 μL of Bst DNA polymerase (1.2 U/mL), 2 μL of Nt.BstNBI (1.0 U/mL), 2 μL of SGI (5 μM), and 2 μL of TMB (1 mM) were added to the mixture. Then, the tubes were put into a TC1000-G thermo recycler (DLAB, Beijing, China) and kept at 60°C for 30 min. The mixture was irradiated by an LED (4W, 470 nm) for 15 min before detecting the absorbance intensity (652 nm).

3. RESULTS AND DISCUSSION

3.1. Construction of the Allosteric Probe. The allosteric probe is designed with a hairpin structure to avoid the nonspecific initiation of subsequent signal cycles and thus ensure high specificity. Therefore, we first investigated the assembly of the allosteric probe and its capability to recognize the CD63 protein on the surfaces of sEVs. The two ends of the allosteric probe are labeled with a fluorophore (FAM) and a quencher (BHQ1), respectively. As shown in Figure 2A, the fluorescence intensity of the linear allosteric probe was significantly higher than that of the hairpin structure allosteric probe, indicating the allosteric probe was successfully assembled into a hairpin structure. When the hairpin structure allosteric probe was mixed with sEVs, the quenched fluorescence signal recovered, implying the allosterism of the probe. However, the fluorescence signal of the allosteric probe

https://doi.org/10.1021/acsomega.5c00016
ACS Omega 2025, 10, 11498−11504

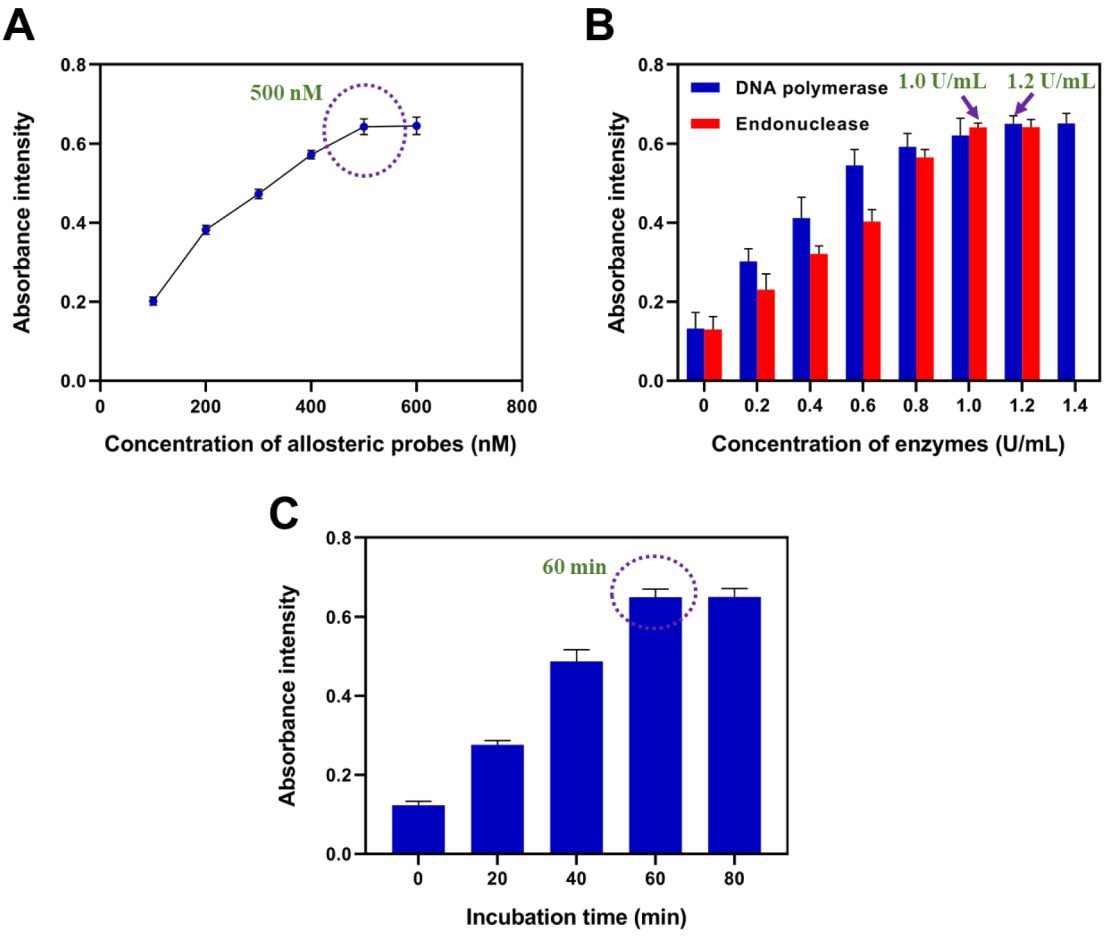

Figure 4. Optimization of experimental conditions. (A) Absorbance intensity of the method when detecting targets with different concentrations of allosteric probe. (B) Absorbance intensity of the method when detecting targets with different concentrations of enzymes. (C) Absorbance intensity of the method when detecting targets with different incubation time.

was low when the allosteric probe was mixed with the recombinant CD9 protein, indicating a high selectivity of the allosteric probe for sEVs. The stability of the allosteric probe was investigated by monitoring the fluorescence signals under different experimental conditions. As shown in Figure S1, the fluorescence signal showed negligible changes when the allosteric probe was added to different solutions, indicating the high stability of the method.

We then tested the capability of the allosteric probe to specifically bind with sEVs by mixing the assembled allosteric probe with sEVs. The results showed that the fluorescence intensity recovered, implying that sEVs could unfold the allosteric probe. As a control, no significant recovery of the fluorescence intensity could be observed when the allosteric probe was mixed with the CD9 protein, indicating that only when sEVs express the CD63 protein on their surface could they unfold the allosteric probe. We then tested the stability of the allosteric probe at different temperatures. The result in Figure 2B showed the allosteric probe stayed stable up to 60 °C, which is sufficient for the target detection.

3.2. Feasibility Analysis. SGI, which can generate fluorescence signals after binding with the double-stranded DNA chains, was used to test the signal cycles. The trigger sequence hybridizes with the "1" section of the allosteric probe in the presence of the target and works as a primer to mediate chain extension. Therefore, the intensity of the SGI signal increased with the assistance of the DNA polymerase. When the EXPAR template was added to the mixture, the SGI signal was further enhanced, indicating the construction of Cycle II, Cycle III, and Cycle IV (Figure 3A). We then tested the feasibility of the whole sensing system by comparing the absorbance intensities of the method when each of the essential components was absent. When monitoring the detection process using the photosensitization colorimetric assay (Figure 3B), only weak TMB absorbance at 652 nm was observed in the absence of the target, due to the low abundance of dsDNA. In the presence of the target, strong TMB oxidation was harvested because of the reserved output dsDNA.

3.3. Optimization of Experimental Parameters. The amplification reaction is significantly influenced by the concentrations of the allosteric probe, DNA polymerase, and endonuclease as well as the detection time of the method. Consequently, the system's critical experimental parameters were optimized to attain the best possible detection efficiency. As illustrated in Figure 4A, the absorbance intensity of the method increased as the concentration of the allosteric probe increased from 100 nM to 500 nM. However, no further increase was observed when the sensing system was incubated with a higher concentration of the allosteric probe. Consequently, the allosteric probe was chosen at a concentration of 500 nM for subsequent experiments. The optimized concentrations of DNA polymerase and endonuclease were 1.2 U/mL and 1.0 U/mL, respectively, as

https://doi.org/10.1021/acsomega.5c00016
ACS Omega 2025, 10, 11498−11504

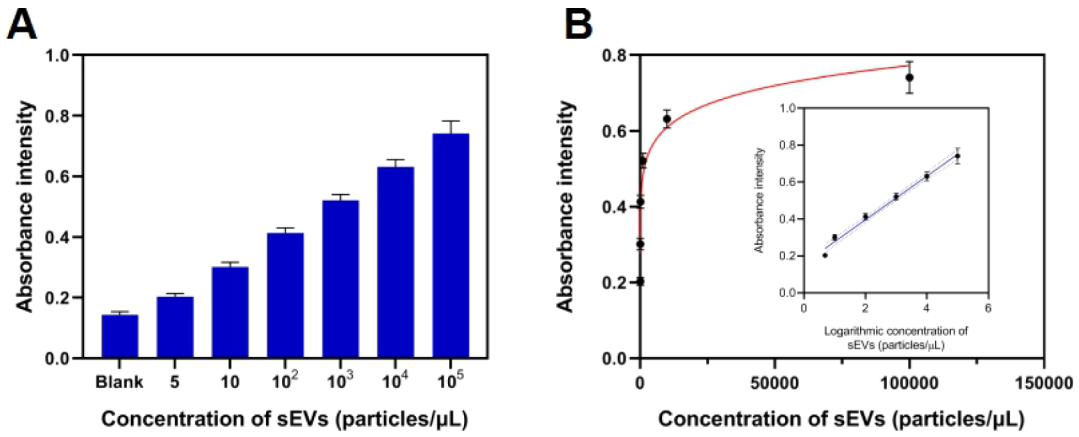

Figure 5. Sensitivity analysis. (A) Absorbance intensity of the method when detecting different concentrations of sEVs. (B) Correlation between the absorbance intensities and the concentrations of target.

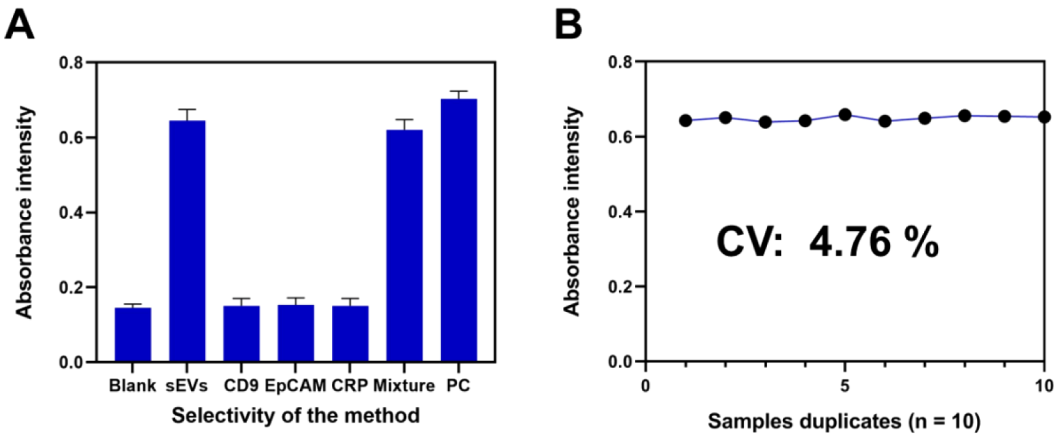

Figure 6. Selectivity and repeatability of the method. (A) Absorbance intensity of the method when detecting target sEVs and interfering molecules. PC, positive control (free CD63 protein). (B) Absorbance of the method when detecting 10 sample duplicates.

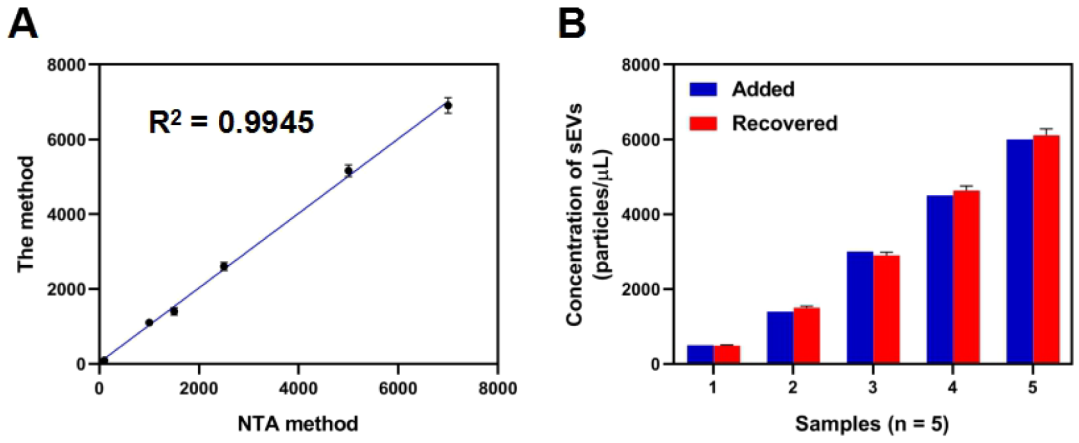

Figure 7. Application potential. (A) Correlation between the calculated sEV concentration by the method and by the NTA method. (B) Recovery test of the method.

demonstrated in Figure 4B. As shown in Figure 4C, the optimal incubation duration of the method was determined to be 60 min.

3.4. Sensitivity Analysis of the Method. The proposed assay was applied for the detection of different concentrations of sEVs following a demonstration of the working principle. As depicted in Figure 5A, the TMB absorbance at 652 nm increased progressively as the concentration of the target increased, exhibiting a linear response within the concentration range of 5 particles/μL to 10^5 particles/μL (Figure 5B). The linear equation was as follows: $A = 0.1184 \times \lg C + 0.1588$ with a high correlation coefficient (R^2) of 0.9936, where A represents the absorbance intensity, and C represents the concentration of the target. The limit of detection (LOD) was calculated at 1.21 particles/μL according to the 3δ rule.

https://doi.org/10.1021/acsomega.5c00016
ACS Omega 2025, 10, 11498−11504

Consequently, this assay provides a high level of sensitivity for the analysis of sEVs.

3.5. Specificity of the Method. The selectivity of a biosensor plays a crucial role in determining its detection capability. We utilized three interfering molecules to assess the discriminative detection capability of the method. The absorption intensities of the method when detecting sEVs can be easily differentiated from those of CD9 protein, EpCAM, and CRP. Evidently, the peak intensity undergoes a decrease of around 82% in the presence of interfering molecules compared to the target at the same concentration (Figure 6A). To evaluate the system's reproducibility, we detected 1.0×10^5 particles/μL of sEVs in 10 duplicate samples. The coefficients of variation (CV) were 4.76% (Figure 6B), indicating that the detection system exhibited good repeatability.

3.6. Application Potential. The number of sEVs in samples was calculated using the NTA (Nanoparticle Tracking Analysis) method and the proposed method to further evaluate the detection effectiveness of the method and its potential in clinical applications. Both approaches have shown a high level of consistency in detecting sEVs (Figure 7A). The stability of the suggested approach was evaluated by testing its performance using commercial serum solution samples mixed with various concentrations of sEVs. As depicted in Figure 7B, by evaluating the characteristic peak values, the approach demonstrated recovery rates of the sEV concentration ranging from 98.68% to 103.6% across various experimental circumstances, demonstrating a high level of stability.

4. CONCLUSION

In conclusion, we illustrated a novel strategy that utilizes an allosteric probe to specifically bind with the CD63 protein for sensitive, label-free, and photosensitization colorimetric sEV detection. In this method, the conformation of the allosteric probe changed in the presence of sEVs, which could then induce four signal cycles to produce substantial double-stranded DNA and be probed by SYBR Green I (SGI). The proposed assay could be engineered to serve as a universal bioassay platform for the detection of other molecules when used in conjunction with other aptamers for probe design. As the photosensitization colorimetric assay necessitates only dsDNA and SGI for signal generation, the assay design is further simplified by the absence of specific DNA structures (e.g., G-quadruplex or i-motif). By combining the polymerase/endonuclease-assisted signal cycles, the proposed method exhibited a low LOD of 1.21 particles/μL, which is superior and comparable to the detection of former sEVs (Table S2). We are confident that this platform will offer a novel approach to the development of biosensors and have potential clinical applications due to its label-free, user-friendly design, and H_2O_2-free signaling.

ASSOCIATED CONTENT

Supporting Information

The Supporting Information is available free of charge at https://pubs.acs.org/doi/10.1021/acsomega.5c00016.

Fluorescence intensity of the allosteric probe (AP) under different experimental conditions (**Figure S1**); sequences of nucleic acid oligonucleotides used in this work (**Table S1**); a brief comparison of the approach with former ones (**Table S2**) (PDF)

AUTHOR INFORMATION

Corresponding Author

Yuyu Chen − *Department of Critical Care Medicine, The First Affiliated Hospital of Army Medical University, Chongqing 400038, China;* orcid.org/0009-0002-6349-9526; Email: Yu0626@tmmu.edu.cn

Authors

Can Wu − *Department of Respiratory and Critical Care Medicine, Chongqing Hospital of Traditional Chinese Medicine, Chongqing 400021, China*

Jingjun Xie − *Department of Geriatrics and Special Service Medicine, The First Affiliated Hospital of Army Military Medical University, Chongqing 400038, China*

Complete contact information is available at: https://pubs.acs.org/10.1021/acsomega.5c00016

Author Contributions

‖J.X. and C.W. contributed equally. Y.C.: supervision, visualization, writing-review, editing; J.X. and C.W. were the co-first authors : methodology, validation, investigation, writing-original draft.

Notes

The authors declare no competing financial interest.

REFERENCES

(1) Cortopassi, F.; Gurung, P.; Pinto-Plata, V. Chronic Obstructive Pulmonary Disease in Elderly Patients. *Clin. Geriatr. Med.* **2017**, *33* (4), 539−552.

(2) Hanania, N. A.; Sharma, G.; Sharafkhaneh, A. COPD in the elderly patient. *Semin. Respir. Crit. Care Med.* **2010**, *31* (5), 596−606.

(3) Kaur, G.; Maremanda, K. P.; Campos, M.; Chand, H. S.; Li, F.; Hirani, N.; Haseeb, M. A.; Li, D.; Rahman, I. Distinct Exosomal miRNA Profiles from BALF and Lung Tissue of COPD and IPF Patients. *Int. J. Mol. Sci.* **2021**, *22* (21), 11830.

(4) Labaki, W. W.; Rosenberg, S. R. Chronic Obstructive Pulmonary Disease. *Ann. Int. Med.* **2020**, *173* (3), ITC17−ITC32.

(5) Rabe, K. F.; Watz, H. Chronic obstructive pulmonary disease. *Lancet* **2017**, *389* (10082), 1931−1940.

(6) Kubo, H. Extracellular Vesicles in Lung Disease. *Chest* **2018**, *153* (1), 210−216.

(7) S, E. L. A.; Mager, I.; Breakefield, X. O.; Wood, M. J. A. Extracellular vesicles: biology and emerging therapeutic opportunities. *Nat. Rev. Drug Discovery* **2013**, *12* (5), 347−357.

(8) Abels, E. R.; Breakefield, X. O. Introduction to Extracellular Vesicles: Biogenesis, RNA Cargo Selection, Content, Release, and Uptake. *Cell Mol. Neurobiol.* **2016**, *36* (3), 301−312.

(9) Bagheri Hashkavayi, A.; Cha, B. S.; Lee, E. S.; Kim, S.; Park, K. S. Advances in Exosome Analysis Methods with an Emphasis on Electrochemistry. *Anal. Chem.* **2020**, *92* (19), 12733−12740.

(10) Jia, Y.; Yu, L.; Ma, T.; Xu, W.; Qian, H.; Sun, Y.; Shi, H. Small extracellular vesicles isolation and separation: Current techniques, pending questions and clinical applications. *Theranostics* **2022**, *12* (15), 6548−6575.

(11) Tang, Q.; Xiao, X.; Li, R.; He, H.; Li, S.; Ma, C. Recent Advances in Detection for Breast-Cancer-Derived Exosomes. *Molecules* **2022**, *27* (19), 6673.

(12) Zhang, Y.; Wang, D.; Yue, S.; Lu, Y.; Yang, C.; Fang, J.; Xu, Z. Sensitive Multicolor Visual Detection of Exosomes via Dual Signal Amplification Strategy of Enzyme-Catalyzed Metallization of Au Nanorods and Hybridization Chain Reaction. *ACS Sens.* **2019**, *4* (12), 3210−3218.

(13) Zhu, C.; Li, L.; Wang, Z.; Irfan, M.; Qu, F. Recent advances of aptasensors for exosomes detection. *Biosens. Bioelectron.* **2020**, *160*, 112213.

(14) Kuang, J.; Fu, Z.; Sun, X.; Lin, C.; Yang, S.; Xu, J.; Zhang, M.; Zhang, H.; Ning, F.; Hu, P. A colorimetric aptasensor based on a hemin/EpCAM aptamer DNAzyme for sensitive exosome detection. *Analyst* **2022**, *147* (22), 5054−5061.
(15) Chen, J.; Xie, M.; Shi, M.; Yuan, K.; Wu, Y.; Meng, H. M.; Qu, L.; Li, Z. Spatial Confinement-Derived Double-Accelerated DNA Cascade Reaction for Ultrafast and Highly Sensitive In Situ Monitoring of Exosomal miRNA and Exosome Tracing. *Anal. Chem.* **2022**, *94* (4), 2227−2235.
(16) Guo, W.; Cai, Y.; Liu, X.; Ji, Y.; Zhang, C.; Wang, L.; Liao, W.; Liu, Y.; Cui, N.; Xiang, J.; et al. Single-Exosome Profiling Identifies ITGB3+ and ITGAM+ Exosome Subpopulations as Promising Early Diagnostic Biomarkers and Therapeutic Targets for Colorectal Cancer. *Research* **2023**, *6*, 0041.
(17) Zhao, X.; Luo, C.; Mei, Q.; Zhang, H.; Zhang, W.; Su, D.; Fu, W.; Luo, Y. Aptamer-Cholesterol-Mediated Proximity Ligation Assay for Accurate Identification of Exosomes. *Anal. Chem.* **2020**, *92* (7), 5411−5418.
(18) Yang, Z.; She, D.; Sun, C.; Gong, M.; Rong, Y. Dumbbell structure probe-triggered rolling circle amplification (RCA)-based detection scaffold for sensitive and specific neonatal infection-related small extracellular vesicle (sEV) detection. *Anal. Methods* **2022**, *14* (15), 1534−1539.
(19) Liu, W.; Li, J.; Wu, Y.; Xing, S.; Lai, Y.; Zhang, G. Target-induced proximity ligation triggers recombinase polymerase amplification and transcription-mediated amplification to detect tumor-derived exosomes in nasopharyngeal carcinoma with high sensitivity. *Biosens. Bioelectron.* **2018**, *102*, 204−210.
(20) Zhang, R. Y.; Luo, S. H.; Lin, X. M.; Hu, X. M.; Zhang, Y.; Zhang, X. H.; Wu, C. M.; Zheng, L.; Wang, Q. A novel electrochemical biosensor for exosomal microRNA-181 detection based on a catalytic hairpin assembly circuit. *Anal. Chim. Acta* **2021**, *1157*, 338396.
(21) Zhou, J.; Lin, Q.; Huang, Z.; Xiong, H.; Yang, B.; Chen, H.; Kong, J. Aptamer-Initiated Catalytic Hairpin Assembly Fluorescence Assay for Universal, Sensitive Exosome Detection. *Anal. Chem.* **2022**, *94* (15), 5723−5728.
(22) Guo, Y.; Cao, Q.; Feng, Q. Catalytic hairpin assembly-triggered DNA walker for electrochemical sensing of tumor exosomes sensitized with Ag@C core-shell nanocomposites. *Anal. Chim. Acta* **2020**, *1135*, 55−63.
(23) Guo, H.; Chen, J.; Feng, Y.; Dai, Z. A Simple and Robust Exponential Amplification Reaction (EXPAR)-Based Hairpin Template (exp-Hairpin) for Highly Specific, Sensitive, and Universal MicroRNA Detection. *Anal. Chem.* **2024**, *96* (6), 2643−2650.
(24) Zhang, Y. P.; Cui, Y. X.; Li, X. Y.; Du, Y. C.; Tang, A. N.; Kong, D. M. A modified exponential amplification reaction (EXPAR) with an improved signal-to-noise ratio for ultrasensitive detection of polynucleotide kinase. *Chem. Commun.* **2019**, *55* (53), 7611−7614.
(25) Ou, X.; Li, K.; Liu, M.; Song, J.; Zuo, Z.; Guo, Y. EXPAR for biosensing: recent developments and applications. *Analyst* **2024**, *149* (16), 4135−4157.
(26) Reid, M. S.; Le, X. C.; Zhang, H. Exponential Isothermal Amplification of Nucleic Acids and Assays for Proteins, Cells, Small Molecules, and Enzyme Activities: An EXPAR Example. *Angew. Chem., Int. Ed.* **2018**, *57* (37), 11856−11866.
(27) Li, X.; Gao, L.; Li, F.; Hou, X.; Wu, P. Universal and label-free photosensitization colorimetric assays enabled by target-induced termini transformation of dsDNA resistant to Exo III digestion. *Chem. Commun.* **2019**, *55* (50), 7211−7214.
(28) Zhang, X.; Huang, C.; Xu, S.; Chen, J.; Zeng, Y.; Wu, P.; Hou, X. Photocatalytic oxidation of TMB with the double stranded DNA-SYBR Green I complex for label-free and universal colorimetric bioassay. *Chem. Commun.* **2015**, *51* (77), 14465−14468.

https://doi.org/10.1021/acsomega.5c00016
ACS Omega 2025, 10, 11498−11504